International Journal of Neural Systems (2021) 2150050 (18 pages)

DOI: 10.1142/S0129065721500507

World Scientific
www.worldscientific.com

Control of Transcranial Direct Current Stimulation Duration by Assessing Functional Connectivity of Near-Infrared Spectroscopy Signals

M. Atif Yaqub
ICFO-Institut de Ciències Fotòniques
The Barcelona Institute of Science and Technology
08860 Castelldefels (Barcelona), Spain
atif.yaqub@icfo.eu

Keum-Shik Hong*
School of Mechanical Engineering, Pusan National University
2 *Busandaehak-ro, Geumjeong-gu, Busan 46241, Korea*
kshong@pusan.ac.kr

Amad Zafar
Department of Electrical Engineering, University of Lahore
Sihala Zone V, Islamabad, Pakistan
amad.zafar@ee.uol.edu.pk

Chang-Seok Kim
Department of Cogno-Mechatronics Engineering
Pusan National University
2 Busandaehak-ro, Geumjeong-gu, Busan 46241, Korea
ckim@pusan.ac.kr

Received 19 August 2021
Accepted 20 August 2021
Published Online

Transcranial direct current stimulation (tDCS) has been shown to create neuroplasticity in healthy and diseased populations. The control of stimulation duration by providing real-time brain state feedback using neuroimaging is a topic of great interest. This study presents the feasibility of a closed-loop modulation for the targeted functional network in the prefrontal cortex. We hypothesize that we cannot improve the brain state further after reaching a specific state during a stimulation therapy session. A high-definition tDCS of 1 mA arranged in a ring configuration was applied at the targeted right prefrontal cortex of 15 healthy male subjects for 10 min. Functional near-infrared spectroscopy was used to monitor hemoglobin chromophores during the stimulation period continuously. The correlation matrices obtained from filtered oxyhemoglobin were binarized to form subnetworks of short- and long-range connections. The connectivity in all subnetworks was analyzed individually using a new quantification measure of connectivity percentage based on the correlation matrix. The short-range network in the stimulated hemisphere showed increased connectivity in the initial stimulation phase. However, the increase in connection density reduced significantly after 6 min of stimulation. The short-range network of the left hemisphere and the long-range network gradually increased throughout the stimulation period. The connectivity percentage measure showed a similar response with network theory parameters. The connectivity percentage and network theory metrics represent the brain state during the stimulation therapy.

*Corresponding author.

The results from the network theory metrics, including degree centrality, efficiency, and connection density, support our hypothesis and provide a guideline for feedback on the brain state. The proposed neuro-feedback scheme is feasible to control the stimulation duration to avoid overdosage.

Keywords: fNIRS; tDCS; functional connectivity; neuromodulation; resting-state; neurofeedback.

1. Introduction

The importance of neurorehabilitation has continued to increase owing to the growing number of patients with brain disorders. Over the last few decades, brain stimulation has been practiced as a rehabilitation therapy to treat brain diseases such as strokes, Parkinson's disease, and various other psychiatric conditions. Our brain tends to restructure or create new neural networks to regain lost or reduced functionalities. Brain stimulation induces or acts as a catalyst in the formation/alteration of such brain functional networks. Transcranial brain stimulation has been augmented to traditional rehabilitation techniques. Transcranial brain stimulation has shown positive rehabilitation effects by facilitating neuroplasticity in healthy participants as well as in patients with mental illness.[1] It has been adopted in adults for many years and recently in children to improve brain functions.[2] Transcranial brain stimulation is provided through magnetic or electrical stimulation (tES).[3] tES is divided into three major methods: transcranial direct current stimulation (tDCS), transcranial alternating current stimulation (tACS), and transcranial random noise stimulation (tRNS).[4,5] These techniques have been proven safe for humans because the stimulation protocols do not cause discomfort to the patients.[6–8] However, the amount of stimulation provided to a subject is still under debate, as different stimulation durations have been employed in previous studies.[9] The efficacy of brain stimulation is also dependent on the subject, as some subjects show more positive effects than others. To provide the right stimulation dosage to a subject, we propose a real-time brain state feedback-based control scheme for stimulation duration using simultaneous neuroimaging and tDCS. The objective of this study is to provide the feasibility of the proposed strategy and recommend the parameters to exhibit the brain state in real-time.

A tDCS device comprises a constant direct current stimulator and electrodes that are attached to the scalp. The small amount of direct current delivered through the scalp enables/enhances cognitive and other brain functions.[4] Currently, different types and sizes of electrodes are being employed, compared to the saline-soaked electrodes used in the past.[6] The device monitors system resistance to ensure the subject's safety and immediately ceases the stimulation when the safety limit is exceeded. The arrangement and polarity of electrodes determine the direction of current flow, which can be used to observe the effects of anodal or cathodal stimulation. Anodal stimulation produces a sub-threshold depolarization that elevates neuronal excitation, whereas cathodal stimulation reduces excitation.[10] The affected regions of the brain exceeded the region under stimulation in many previous studies.[11] tDCS was applied in the prefrontal cortex of the human brain to investigate its effects on working memory,[12] motor plasticity, excitability, and learning,[9,11] psychiatric symptoms,[9] functional connectivity,[13] and hemodynamics.[14,15] To develop an understanding of the current path during stimulation and the spread of the field generated in brain regions, direct measurements from the head are not possible. Therefore, simulations were carried out to determine the stimulation effects in adults and children. Researchers performing modeling and electric field simulations have used electrodes of different sizes and shapes to determine the most advantageous montage.[16] A montage with multiple cathodes arranged in a ring around an anode as the center was useful in containing the electrical field to the targeted brain area.[17,18] This high-definition (HD) montage, consisting of multiple electrodes that focus the effects of stimulation at the desired brain region, is defined as HD-tDCS.[19] Comparing the conventional and focal effects of stimulation showed that HD-tDCS-generated neuroplasticity remained for longer periods.[20]

Recently, functional near-infrared spectroscopy (fNIRS), which can be used to emit multiple wavelengths of near-infrared light on the brain, has been

used to monitor neuronal activation. For elucidating neuronal firing, fNIRS measures the changes in oxygen metabolism that are derived from the neurovascular coupling. The chromophores of oxyhemoglobin (HbO) and deoxyhemoglobin (HbR) describe the oxygenation state of brain tissues. fNIRS has been used in a wide range of subjects covering all ages, from infants to the elderly.[21–23] A broad spectrum of applications involving patients and healthy populations has employed fNIRS as a neuroimaging modality.[24,25] The features of this modality enable its utilization in brain–computer interfaces.[26,27] In addition, it can simultaneously measure the changes in blood oxygenation during stimulation. A combination of fNIRS and tDCS is favorable as the stimulation does not produce noise in the acquired neuroimaging data. The electric fields and flowing currents produce interference with other commonly used neuroimaging modalities, such as functional magnetic resonance imaging and electroencephalography. Recent advances in fNIRS have enabled battery-operated, wearable, and low-cost devices comparable to stimulation devices.[28]

Functional connectivity is defined as the correlation of time-series data from different brain regions acquired using any neuroimaging techniques.[29–33] fNIRS has been actively used to measure cognitive capacity by analyzing functional connectivity in the prefrontal cortex.[34,35] The brain state can be modeled in nodal networks, representing the information flow and connectedness of different regions. The loss of or reduced connectivity results in decreased cognition capacity and is linked to various brain disorders requiring rehabilitation.[36,37] Using the Pearson correlation coefficient of the fNIRS channels, functional connectivity capacity and capability have been explored using the network theory.[38,39] The network theory metrics provide a comprehensive quantification for the network under study and robustly track the changes in real-time, which are critical for expressing the enhancement in brain state.[40,41] The real-time tracking of brain state has much significance for the evolving tele-neuromodulation.[42] Bedsides, neuromonitoring and neurorehabilitation can be achieved using a combination of wearable fNIRS and tDCS devices.

This paper provides the feasibility of our proposed strategy for controlling the stimulation duration during a brain stimulation session. In the HD-tDCS protocol, the subject's brain signals from both hemispheres of the prefrontal cortex are measured using fNIRS. fNIRS optodes are spread over the scalp of both hemispheres, while the HD-tDCS montage containing one anode and four cathodes is attached to the right hemisphere. The blood chromophore to be analyzed can be monitored in real-time using fNIRS. Pearson's correlation coefficient is computed for all channel combinations to generate the functional connectivity maps in order to continuously evaluate the brain state of the entire prefrontal cortex. We hypothesize that the improvement in resting-state functional connectivity would reduce after a certain stimulation duration and that further stimulation would not improve the brain state significantly. Therefore, further stimulation for the subject under study should be stopped in that session to avoid overdosage. To the best of our knowledge, this is the first study considering fNIRS to develop a control scheme for the stimulation duration of tDCS.

2. Materials and Methods

2.1. *Participants*

For analyzing the resting-state functional connectivity during stimulation, 20 male subjects with short hair were recruited. This study does not focus on evaluating gender-based effects; therefore, male subjects are selected to ensure uniform head sizes. Short hair allows for more accessible contact between the scalp and optodes. The subjects reported themselves to be healthy and not under any medications. Their medical histories did not include any neurological illness, psychiatric impairment, or brain injuries. We explained the experiment and the risks involved in electrical stimulation to the subjects; they were asked to inform the experimenter to stop the stimulation on experiencing high levels of discomfort. The subjects were also asked to avoid caffeinated drinks such as coffee or tea before the experiment. The subjects provided written consent for participation in this study and received compensation after completing the study. The experiment was completed for 15 subjects (mean age [standard deviation]: 28.5 [2.5] years) because one subject needed to withdraw from the experiment due to a severe itching sensation during stimulation, while four subjects had improper placement of the stimulating electrodes. The subjects were the graduate students of Pusan

National University with ages ranging between 25 and 33 years. Every subject had at least a university degree. The experimental paradigm was approved by the Human Research Ethics Committee of Pusan National University and conformed to the latest Declaration of Helsinki.[43]

2.2. *Experimental paradigm*

The experiment involved 10 min of stimulation with the subject in the resting state with simultaneous neuroimaging. The subjects were seated on an examination chair with the backrest in the reclining position. Each subject was allowed to adjust the reclining angle to ensure comfort. For all the subjects, the leg rest was oriented in the horizontal position. Once the subject was seated appropriately, his forehead was marked for attaching the stimulation electrodes. A guide was created to mark the electrode locations with reference to the nasion position of the International 10–20 System. Self-adhesive electrodes are placed on the forehead for exploring the benefits of combining fNIRS and tDCS. A probe composed of polyurethane foam was used to maintain the imaging optodes and stimulating electrodes over the complete prefrontal cortex, as shown in Fig. 1. Similar head size was helpful in the experimental setup and provided good optode–scalp coupling. Furthermore, we used a Velcro band to tighten the probe according to the subject's head. The 10-min stimulation commences with a ramp-up phase of 15 s, where the stimulation current rises linearly from zero to the set-point. A steady current flowed from the anode to the four cathodes for 9 min and 30 s. Lastly, stimulation

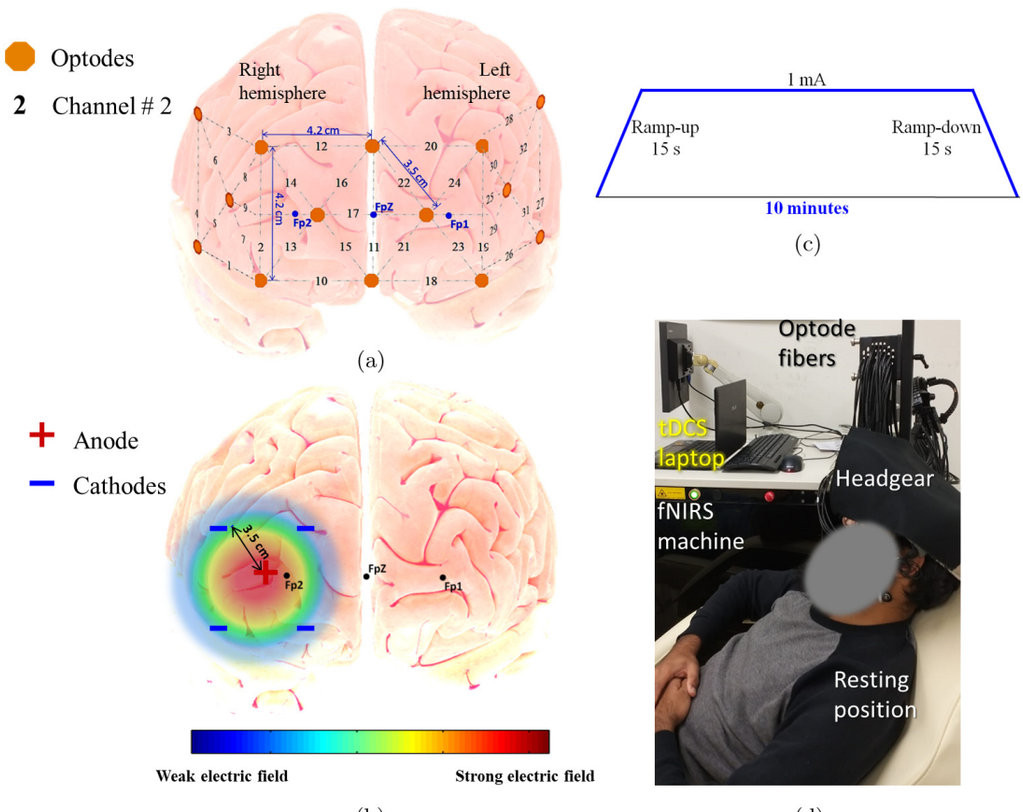

Fig. 1. (a) fNIRS channel configuration. The numbers represent fNIRS channels. Each channel has a source and a detector. (b) HD-tDCS montage on the right hemisphere. The anode with a plus sign in the center is surrounded by four cathodes with a minus sign. The color gradients show the simulated stimulation intensity. (c) tDCS current profile for the experiment. (d) An experimental setup where the subject is resting in Fowler's position with equipment attached on the head and covered by a black cloth to avoid ambient light.

ended with a ramp-down phase of 15 s, where the current declined linearly from the setpoint to zero. Subjects were instructed to keep their eyes open and remain awake throughout the experiment.

2.3. *Electrical stimulation*

tDCS is administered to subjects using the battery-operated device, Starstim tCS System, from Neuroelectrics, Barcelona, Spain. The device is controlled using Neuroelectrics® Instrument Controller 2.0 (Neuroelectrics), running on a Windows-based laptop. The software communicates with the device through Bluetooth. The stimulation montage is configured using this software. Five of the eight electrodes are employed in an HD montage, where a single anode is surrounded by a ring of four cathodes, as shown in Fig. 1. This montage focuses on the effects of the applied stimulation by limiting the electric field within the ring of cathodes.[18,19,44] Disposable foam electrodes with a conductive, adhesive hydrogel, procured from Medtronic, Minneapolis, USA, are used for the experiment. Circular electrodes of 1-cm diameter are used in this study. The ring montage for HD-tDCS features a radius of 3.5 cm and is placed to target the right hemisphere of the prefrontal cortex. The current intensity is set using the software, such that the anode supplies one mA and each cathode receives 0.25 mA on average. The device includes built-in safety features that abort the stimulation when the impedance at any electrode interface changes due to improper contact or other unforeseen circumstances. In this manner, the desired current is supplied steadily, with the electrode voltages maintained at a safe level.

2.4. *Neuroimaging system and optode configuration*

The fNIRS-based continuous-wave neuroimaging system (DYNOT) with 32 optodes, from NIRx Medical Technologies, USA, is utilized in our experiments. Each optode can emit two wavelengths (760 nm and 830 nm) of light and simultaneously receive incoming near-infrared light. A total of 14 optodes spread over the forehead of the subject and covering the complete prefrontal cortex result in a total of 32 fNIRS channels. The optodes are embedded in the polyurethane probe that conforms to the scalp in a comfortable manner. Each optode pair provides raw time-series signals for both wavelengths, resulting in HbO and HbR for each channel. The vertical and horizontal distances between the optodes are set as 42 mm, whereas the diagonal distance is set as 35 cm, as shown in Fig. 1. The data acquisition rate during the experiments is 1.81 Hz.

2.5. *fNIRS data preprocessing*

The raw data files are used to convert light intensities to changes in the HbO and HbR concentrations. Subsequently, the NIRS-SPM software is used for conversion to blood chromophores, according to the modified Beer–Lambert law.[45] The values of the differential path length factor used for wavelengths of 760 nm and 830 nm are 7.15 and 5.98, respectively. The extinction coefficients of HbO and HbR are 1.4866 and 3.8437 for 760 nm and 2.2314 and 1.7917 for 830 nm, respectively. The fNIRS signal is affected by the heartbeat rhythm, respiration pattern, and Mayer waves. Therefore, the HbO and HbR signals are filtered using a fourth-order Butterworth low-pass filter with a cut-off frequency of 0.1 Hz, using MATLAB® (The MathWorks Inc., Natick, MA, USA).[44] The filtered signal of HbO is used for further analyses as it is more reliable and sensitive than HbR.[22] For the baseline correction of each channel, curve fitting with a fourth-order polynomial is employed.[46] The fitted curve is subtracted from the original signal to obtain the corrected signal. The signal means are computed for each channel using data from all the subjects to eliminate the effects of variability in the fNIRS data. The experiment was conducted while the subject was resting in Fowler's position and did not perform any movements. Therefore, the data did not require preprocessing for movement artifact removal.

2.6. *Brain functional network*

Several groups of neurons from different brain regions are fired when performing a task. The brain regions that exhibit harmonized neuronal firing are considered to be connected for that specific task. Functional neuroimaging reveals these functional networks in comparison to the brain connectome acquired via structural neuroimaging. For visualizing functional connectivity, the brain is considered as a particular type of network with a set of highly connected nodes, along with some isolated nodes.

Functional networks associated with different functions also exist in the resting state, as the areas that are activated simultaneously during a task also hum synchronously.[47] Therefore, the resting-state functional network, also known as the default mode network, is essential for gauging cognitive capability. In fNIRS, each channel spans a brain area that is considered a single node. In this study, a functional brain network with 32 nodes from the prefrontal cortex is explored. The HbO signals of all the subjects were averaged to negate the effect of subject-to-subject variability in the data. The averaged HbO signal from each channel is used to generate a connectivity matrix. In this study, for the 32 channels used, the connectivity matrix, including both hemispheres of the prefrontal cortex, has a size of 32×32. The connectivity matrix is assembled by computing the Pearson's correlation coefficient among all channels according to the following equation:

$$r = \frac{\sum (x_i - \overline{x})(y_i - \overline{y})}{\sqrt{\sum (x_i - \overline{x})^2 \sum (y_i - \overline{y})^2}},$$

where r is the correlation coefficient, x_i represents the x-variable in a sample, $\overline{x}$ represents the mean of the x-variable, y_i represents the y-variable in a sample, and $\overline{y}$ represents the mean of the y-variable. The Pearson's correlation coefficient indicates the synchronization between two channels. A higher synchronization is represented by a higher correlation value between the channels. Each element r in the connectivity matrix represents the connection strength between channels x and y. The diagonal elements have a value of 1 as they represent the correlation of a channel with itself. This resting-state brain network does not express the direction of the connection; therefore, the upper and lower diagonal matrices are similar, as the correlation between x and y or y and x are identical. To quantify functional connectivity, we compute the connectivity percentage for each network at every second. The connectivity percentage is calculated by dividing the sum of the binary matrix from its maximum possible sum. For the short-range and complete prefrontal networks, the connectivity percentage is calculated using elements of the triangular matrix under the main diagonal of their corresponding matrices. Whereas, for the long-range network, the connectivity percentage is computed using all elements of the matrix. A fully connected network where all nodes are connected to every other node is said to have a connectivity of 100%.

The connectivity map was calculated every second using an increasing window, where the window length increases linearly with time. The window progressively increases its size with time to accommodate new data points and retain the previous data points since the onset of the experiment. With this scheme, we keep the complete history of the brain state in consideration while updating the current state such that any momentary synchronized variations cannot be considered an enhanced brain state. The initial window length is set as 3 min to acquire a sufficient number of data points for computing the correlation value. The correlation maps computed at every second during the stimulation are treated as images.

For generating brain functional networks, valid connections are decided based on the correlation coefficient value. A connection is accepted when the correlation value exceeds the threshold of 0.8. If the threshold is set to a lower value, the specious connections will be included in the results that should be avoided. The inclusion of these connections can largely exaggerate the results of the study by hampering the legitimate functional network.[48] On the other hand, if the threshold value is set to very high, the change in connectivity cannot be fully visualized, as there may be some connections that are broken by connectivity. Using the threshold mechanism, the correlation matrix is converted to a binary connectivity matrix, where 1 represents a connection and 0 represents a lack of connection.

2.7. *Network theory*

The brain network connections are categorized as short- and long-range connections. Short-range connections are formed within a hemisphere; two short-range networks are formed for the right and left hemispheres separately. Long-range connections are formed between the channels of the right and left hemispheres. Therefore, a total of four networks are formed: short-range network of the right hemisphere, short-range network of the left hemisphere, long-range network of connection between the hemispheres, and complete network of the prefrontal cortex. Network theory metrics are employed to explore the properties of the default mode network

using the FC-NIRS toolbox in MATLAB®.[49] Degree centrality, global degree, connection density, nodal efficiency, network efficiency, local efficiency, clustering coefficient, network modularity, network assortativity, and nodal betweenness are utilized to analyze the effects of HD-tDCS. The global degree of the short-range network for the right hemisphere describes the effects in our region of interest (ROI). Degree centrality shows the highest effect of stimulation over the local brain region. Nodal efficiency gauges the effectiveness of each node for communication within the brain functional network. Network efficiency provides the overall communication efficiency of the functional network. Local efficiency provides the capacity of information flow within a local region. The clustering coefficient measures the tendency of nodes in a graph to form groups. Modularity shows the density of connections when the network is divided into subnetworks. Assortativity determines the tendency of nodes to have connections with only similar nodes. The betweenness of a node illustrates its presence in the shortest paths of the network. These network metrics can efficiently describe the state of any network. Together these metrics explain the structure, the colonization, and communication efficiency at a given instant of time.[45] As we have considered the brain state in the form of a network, the connectivity percentage along with these metrics can robustly provide the changes occurring in the brain state during the stimulation therapy.

2.8. *Statistical analyses*

The changes occurring due to the application of HD-tDCS were analyzed statistically to categorize them as significant or non-significant. The brain functional networks are the correlation matrices that are generated as images with corresponding sizes. Jet colormap was used in the MATLAB® for making the correlation map. Therefore, image-based differences are calculated for the correlation maps. Correlation and structural similarity indices are suitable for measuring significant differences as the correlation maps is a boxed image, unlike the usual pictures.[50] In this study, the image sizes are much smaller than the typical pictures of humans and or scenic environments. The maximum size is 32×32 for the whole prefrontal network. For the network theory results, the network size varies from the full prefrontal network to the short- or long-range networks, the method to evaluate significant improvements/differences should accommodate the sample size. Therefore, repeated measures t-test and unpaired t-test are used for the network theory metrics of all networks accordingly.[39] A confidence interval of 95% was used to declare significant changes.

2.9. *Neurofeedback*

The control of the stimulation duration can be accomplished by performing neuroimaging in parallel with HD-tDCS. If the desired brain state is

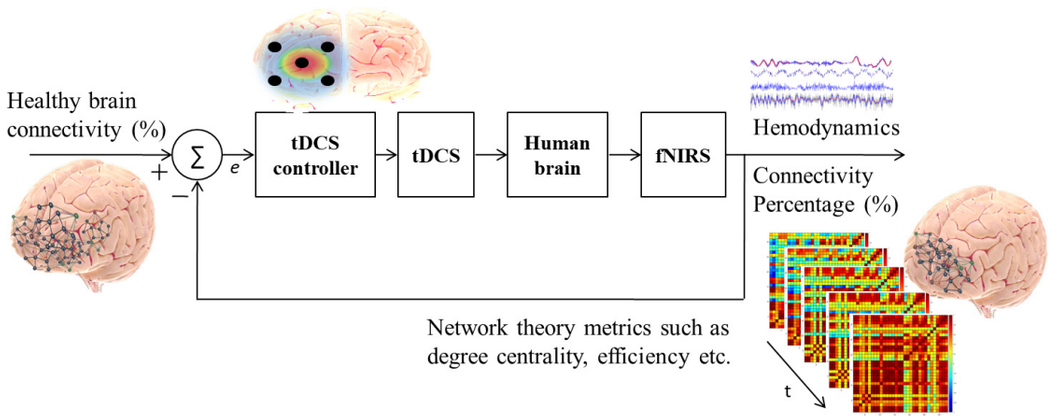

Fig. 2. Block diagram for the proposed closed-loop methodology for controlling stimulation duration using neurofeedback from functional connectivity. Network theory and proposed connectivity percentage can be used to provide the feedback about brain state. The current brain state is continuously compared to the desired state, and the stimulation is stopped when the current brain state is equal to desired brain state.

already known in terms of the connectivity percentage, a network theory metric, or a combination of metrics, the stimulation can be aborted when this known state is achieved. The closed-loop block diagram for controlling the stimulation duration is shown in Fig. 2. Currently, fNIRS devices provide blood chromophores in real-time. The concentration changes in HbO generate connectivity maps that reveal the underlying brain functional network in real-time. This closed-loop simultaneous neuroimaging and transcranial brain stimulation can prevent the overdosing of HD-tDCS to the brain. To this end, analyses of all brain functional networks, including the ROI, are performed to understand the changes occurring during brain stimulation.

If the desired changes in functional connectivity do not occur, the stimulation session can be terminated. In this study, we provide the feasibility of the neurofeedback along with hypothesis that the brain state of the targeted region improves continuously only for a certain stimulation duration, after which it ceases, or any further enhancements become insignificant.

3. Results

The effects of HD-tDCS are evaluated by quantifying the resting-state functional connectivity. Figure 3 shows the connectivity percentage of the functional brain network in the complete prefrontal cortex and subnetworks of short- and long-range connections. Connectivity percentage continues to increase during stimulation. The ROI shows a sharp increase during the first 6 min of stimulation. Although a significant difference ($p < 0.05$, repeated measures t-test) is observed between the connectivity percentage at 3 and 6 min, there is no compelling change in the connectivity percentage over the last 4 min for the ROI. In contrast, the resting-state functional connectivity in the left hemisphere is not affected significantly by the stimulation. The left hemisphere shows a gradual decrease in connectivity percentage, which is regained in the last 3 min of stimulation. Therefore, no considerable effect is observed in the brain state of the left hemisphere. The connectivity percentage for the long-range network in the complete prefrontal cortex exhibits a constant increase that commenced after approximately 4 min of stimulation and continued till the end of the stimulation.

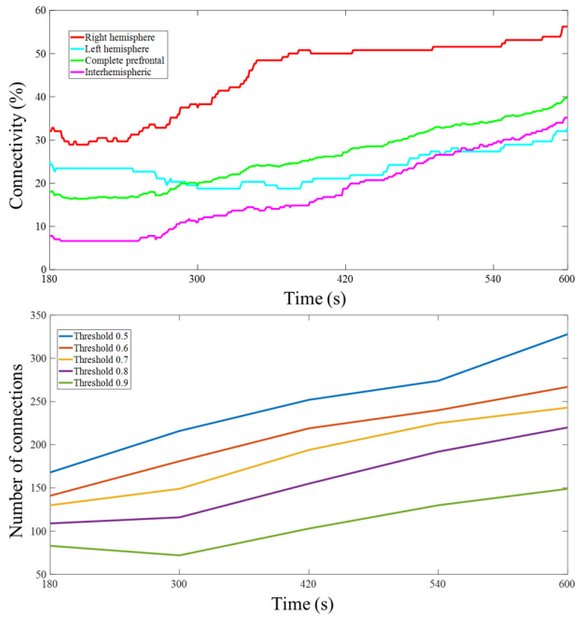

Fig. 3. (Color online) The trend of connectivity percentage for all networks and the trend for number of connections for complete prefrontal network at different threshold levels from 3 min to the end of stimulation.

Figure 3 also shows the total number of connections in the complete prefrontal cortex at threshold levels of 0.5, 0.6, 0.7, 0.8, and 0.9. An increasing trend is observed in all threshold values. The number of connections reduces as the threshold value increases as observed in our previous study.[18]

Figure 4 shows a graphical illustration of the developing connections and their locations in the prefrontal cortex. Each line between two nodes represents a channel; the lines do not denote the strength of the connection and only exhibit a binary network. Every connection in this representation has a correlation coefficient exceeding the threshold value of 0.8. Figure 4 shows the correlation maps for each network at the marked timestamps below the time axis. The connection strength continues to increase for most connections in all the networks. A correlation coefficient of 0.94 and a structural similarity index of 0.81 are noted between the right hemisphere maps obtained at 7 min and 10 min. The maps obtained at 3 min and 7 min showed a structural similarity index of 0.58 and a correlation value of 0.62. The structural similarity index between the initial and final correlation maps of the left hemisphere, interhemispheric, and complete prefrontal cortex are 0.46,

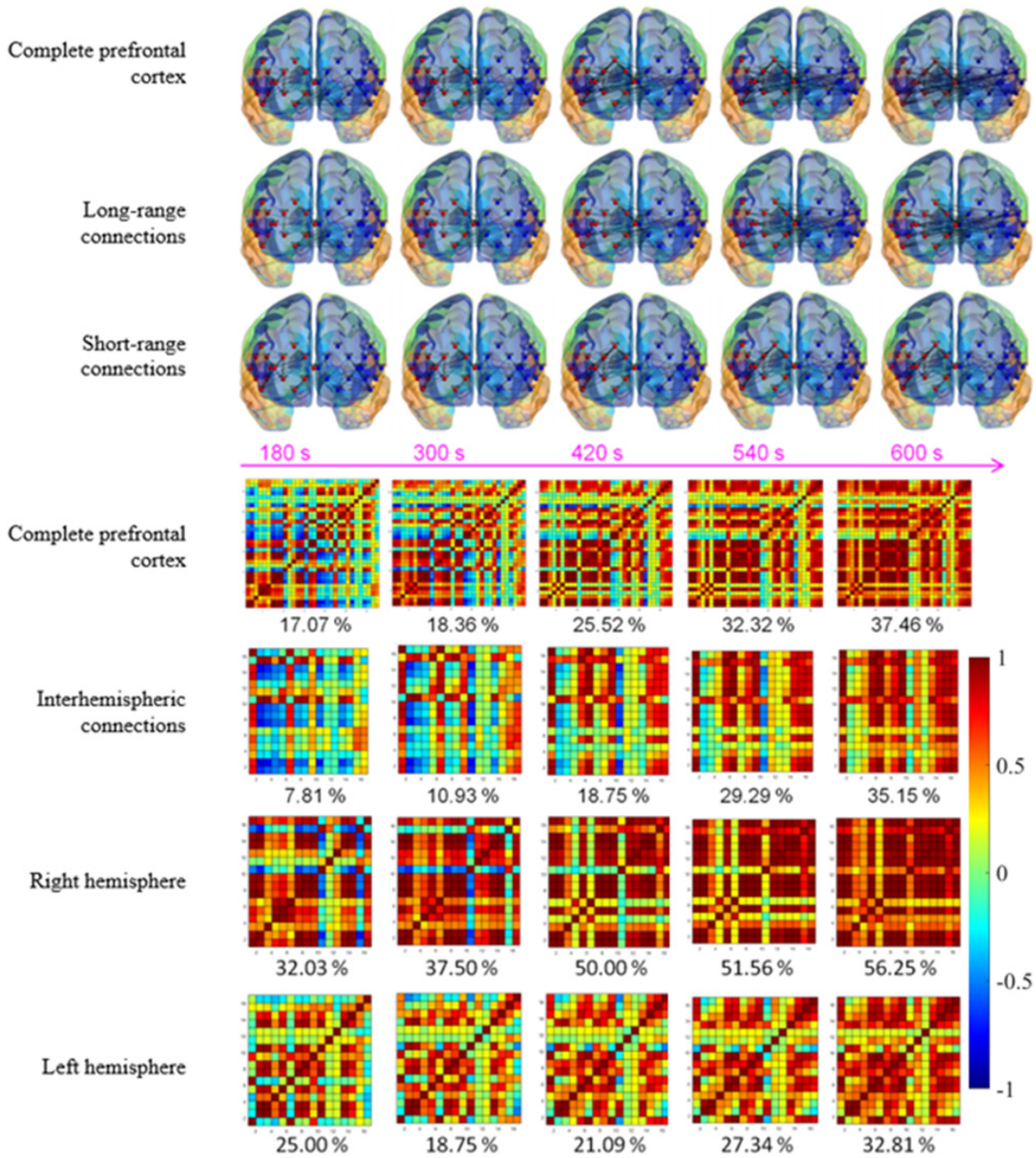

Fig. 4. Changes in connections of functional networks above the time axis and correlation maps with marked connectivity percentage below the time axis. The scalebar is same for all figures.

0.03, and 0.2357, respectively. The correlation coefficient values between the initial and final correlation maps were 0.57, 0.57, and 0.56 for the left hemisphere, interhemispheric, and complete prefrontal cortex, respectively.

The network theory metric of degree centrality is measured for all nodes at each stage during the application of HD-tDCS, as shown in Fig. 5. The complete network in the prefrontal cortex shows the highest degree and an increasing trend of degree centrality. The short-range network of the right hemisphere also shows an increasing trend, although the slope is higher during the initial 7 min of stimulation. The short-range network of the left hemisphere

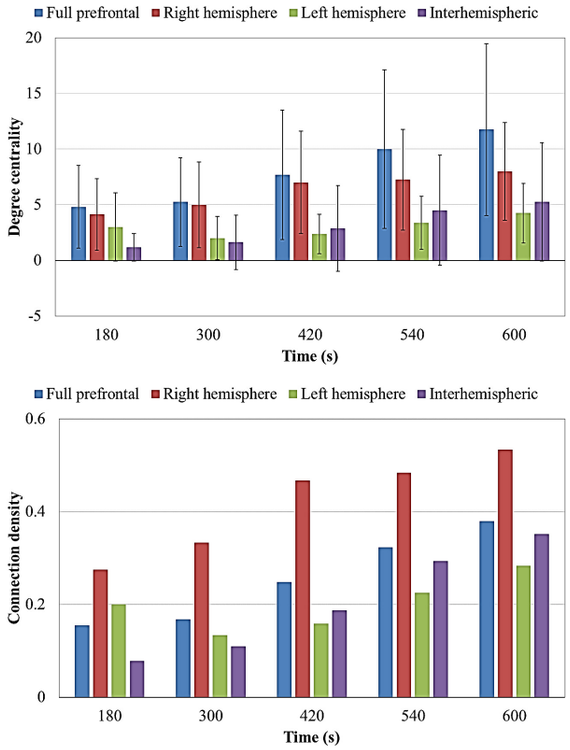

Fig. 5. Degree centrality with standard deviations and connection density of all functional networks.

shows a reduction in degree centrality during the first 7 min of stimulation, whereas the remaining half exhibits a slow increase. The long-range network had few connections initially; however, new connections spawned throughout the stimulation. More long-range connections are developed during the last minutes of the stimulation. The repeated measures t-test shows a significant difference between the degree centrality at 3 min and 7 min ($p < 0.01$). In contrast, no significant difference is observed between 7 min and 10 min of stimulation ($p > 0.05$) for the short-range network of the right hemisphere. The average degree centrality of the stimulated nodes is greater than that of the unstimulated nodes in the short-range network of the right hemisphere. The average degree centrality of the stimulated and unstimulated nodes after 7 min of stimulation corresponds to 8 and 5.33, respectively. The average degree centrality over the complete stimulation period for the stimulated nodes and unstimulated nodes was 7.08 and 4.93, respectively. It is important to note that the complete prefrontal cortex contains 32 nodes, creating connections with all other nodes. In contrast, each node in the short-range can create 15 connections, while each node in the long-range network can create 16 connections. The connection density for each network is also measured. It encompasses the limit of connections that each node can form. Figure 5 shows that the right hemisphere has the highest connection density. During the first 7 min of stimulation, the increase in connection density for the right hemisphere is higher than that during the last 3 min. The connection density of the interhemispheric network increases significantly and is almost similar to that of the complete prefrontal network. An unpaired t-test is used to show that there exists a significant difference between the short-range network of the stimulated right hemisphere and that of the unstimulated left hemisphere ($p < 0.05$). The short-range network of the right hemisphere is significantly different ($p < 0.05$) from the remaining networks in terms of the connection density. There is no significant difference ($p > 0.05$) between the connection densities of the complete prefrontal network, long-range network, and short-range network of the left hemisphere.

The global efficiency for each network is represented in the form of bar plots in Fig. 6. The global efficiency of the right hemisphere is the highest among all the networks. The unpaired t-test indicates a significant difference ($p > 0.05$) of global efficiency for the short-range network of the right hemisphere from the short-range network of the left hemisphere and the long-range network. The long-range network, complete prefrontal network, and short-range network of the left hemisphere show no significant difference ($p > 0.05$). Interestingly, only the long-range network showed a significant increase in the local efficiency, as shown in Fig. 6. The enhancement in the local efficiency for the long-range network surpasses that for all other networks. The clustering coefficient also shows similar behavior (Fig. 6), as indicated by the local efficiency. The local efficiency and clustering coefficient showed no significant difference between the short-range network of the right hemisphere and complete prefrontal network, and the short-range network of the left hemisphere and long-range network ($p > 0.05$, unpaired t-test), while the other cases showed significant differences ($p < 0.01$, unpaired t-test). It is noteworthy

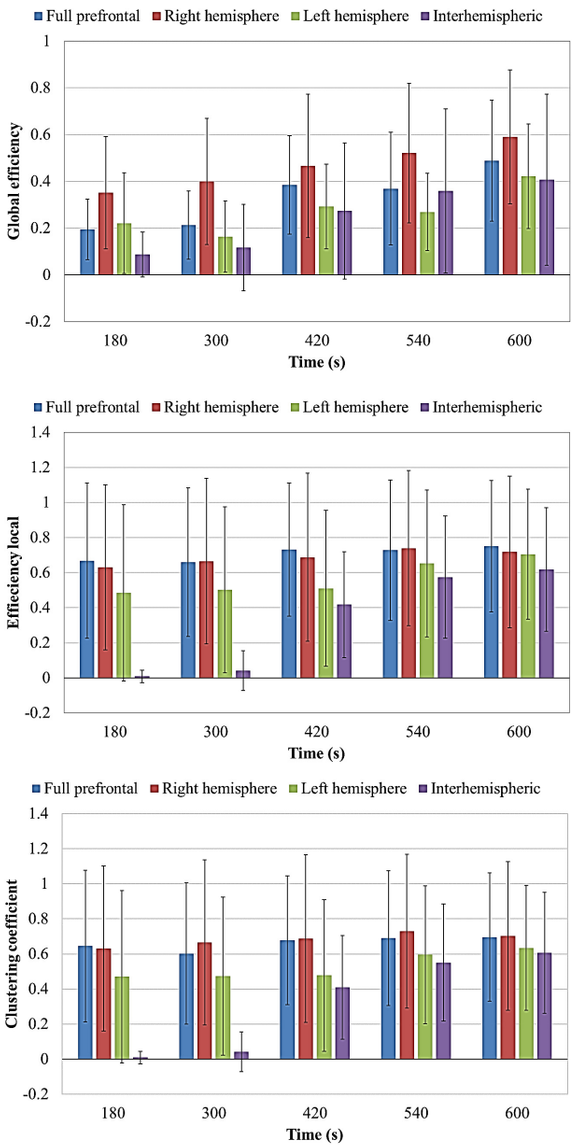

Fig. 6. Global efficiency, local efficiency, and clustering coefficient with the standard deviations of all functional networks during the stimulation duration.

that within the short-range network of the right hemisphere, the average nodal efficiency of the stimulated nodes is higher than that of the unstimulated nodes. The average nodal efficiency of the stimulated nodes after 7 min of stimulation is 0.53, whereas it is 0.35 for the unstimulated node. The further 3 min of stimulation after the 7 min did not show any significant difference as the stimulated nodes had 0.51

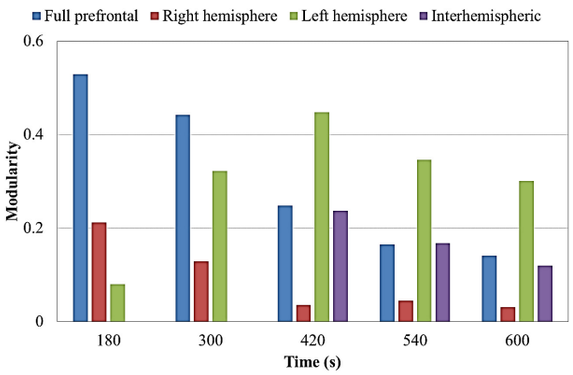

Fig. 7. Modularity of all networks during the stimulation duration.

while the unstimulated nodes had 0.38 average nodal efficiency.

The modularity of all networks is calculated and is shown in Fig. 7. The modularity shows a decline for the complete prefrontal network and the short-range network of the right hemisphere. The decline in the short-range network of the right hemisphere exhibits a shear slope during the initial 7 min, whereas the value over the last 4 min remains almost identical. The modularity trend of the short-range network of the right hemisphere shows a significant difference ($p < 0.05$, unpaired t-test) between the full prefrontal network and the short-range network of the left hemisphere. The short-range network of the left hemisphere exhibits an unexpected behavior where the value increases significantly during the first 7 min, followed by a relatively slower decrease during the remaining stimulation period. The modularity of the short-range network of the left hemisphere shows no significant difference ($p > 0.05$, unpaired t-test) from the complete prefrontal network. Still, it shows a significant difference ($p < 0.05$, unpaired t-test) compared to the long-range network.

The assortativity coefficient, shown in Fig. 8, of the complete functional brain network of the prefrontal cortex exhibits a constant increase throughout the stimulation period. The short-range network of the right hemisphere shows an increasing trend, reaching its maximum value after 7 min of stimulation and exhibiting a perfect assortative mixing pattern. The short-range network of the left hemisphere shows a variable response that increases at the very last stages of the stimulation. Its assortativity coefficient shows a highly negative value

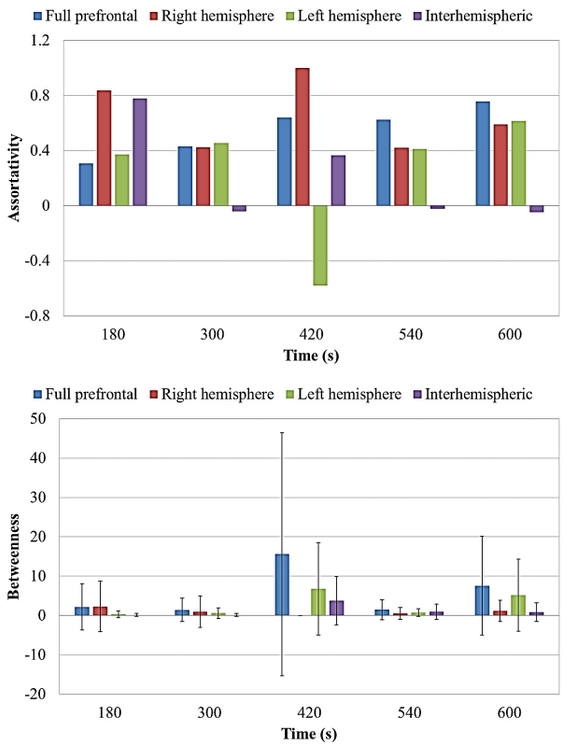

Fig. 8. Assortativity and betweenness with the standard deviations of all networks during the stimulation duration.

after 7 min of stimulation. Furthermore, the long-range network presents a decline in the assortative mixing pattern as the stimulation time increases. The long-range network ends slightly toward the negative side, becoming marginally disassortative. Betweenness centrality is measured for all the nodes in each network. The mean betweenness value for each network is computed and shown in Fig. 8. Random behaviors without any consistency are observed for each network. There is no significant difference among the assortativity coefficients and the mean nodal betweenness of all networks ($p < 0.05$, unpaired t-test).

4. Discussion

The use of neuromodulation using electric stimulation has the potential for the rehabilitation of various impaired/lost brain functions. However, controlling the stimulation duration is challenging and depends on many variables related to the subject. In this study, we evaluated the duration of HD-tDCS for a targeted brain region. This is the first study to propose a limiting mechanism for the stimulation duration of a diseased brain. We evaluated the effects of HD-tDCS on the right prefrontal cortex by measuring the resting-state functional connectivity in the prefrontal cortex over 10 min of stimulation. After preprocessing, the acquired fNIRS data to remove noise from various sources, correlation maps that quantitatively measure the resting-state functional connectivity were computed using the averaged HbO signal. The results showed a strong correlation (threshold = 0.8) between different pairs of channels that can be considered to be connected. The brain functional network for the complete prefrontal cortex was divided into subnetworks based on the connectivity percentage between channels. The independent short-range networks of the right and left hemispheres featuring connections within a hemisphere, long-range networks with connections between the channels of the right and left hemispheres, and the complete prefrontal cortex network incorporating short- and long-range connections were investigated based on network theory properties. The results show improvements in brain functional networks with increasing stimulation duration. The ROI exhibited a significant enhancement in the brain state during the initial 7 min. However, no significant difference in the brain state was observed in the latter 3 min. Therefore, it can be assumed that the improvements in the brain state were close to saturation and that further stimulation should be avoided to prevent overdosing. In this manner, the stimulation duration can be controlled using the proposed neurofeedback methodology.

Several studies have shown that many executive functions that are essential for daily activities depend on the neuronal circuits of the prefrontal cortex.[51,52] Therefore, any loss in the cognition capability of a diseased brain can be restored by rehabilitating the prefrontal cortex. The default mode prefrontal cortex network has been linked to diverse psychiatric conditions.[37,53,54] Even though these studies provided evidence for the loss of connections in functional brain networks, they do not quantify the reduced or altered functional connectivity. Therefore, in this study, we introduced the concept of connectivity percentage based on the connectivity matrix. The connectivity percentage showed that the

improvement in the functional brain network was in agreement with the results obtained through the established connectivity analyses using network theory. The right hemisphere of the prefrontal cortex is associated with cognition, emotion, decision-making, and stress.[55–58] The anodal stimulation of the right hemisphere was shown to affect these functions positively.[59–61] In addition, an increase in resting-state functional connectivity was observed when administering HD-tDCS. The increase was reflected in the entire functional network of the prefrontal cortex, including the short- and long-range networks.

In this study, the short-range network of the ROI showed rapid improvements, as compared to the other networks, especially during the initial 6 min of stimulation. This was in agreement with our hypothesis that the brain state does not improve further once a saturation level is achieved. It is evident that the short-range network of the left hemisphere, the unstimulated hemisphere, and the long-range interhemispheric network showed a continuous increase in connectivity for the duration of the stimulation. It can be expected that this trend would have continued had the stimulation duration been extended beyond the set 10 min. The expeditious change in the stimulated hemisphere can be associated with the focal effect of HD-tDCS, which was also observed in previous studies.[18,44] The observed global increase in functional connectivity during stimulation was similar to that in other studies applying tDCS to various brain regions.[62,63]

For several years, neuroscientists have used network theory analyses to evaluate functional connectivity in brain functional networks.[64,65] We utilized the commonly used metrics of network theory to analyze and compare all the networks. The degree centrality results for all networks coincided with the results of connectivity percentage. The global analysis of degree centrality showed that the average number of connections between the nodes in the network increased throughout the stimulation duration. The nodes of the stimulated right hemisphere showed higher values, but the increase in connectivity was also prominent for the complete prefrontal and long-range networks. This is because the short-range network of the left hemisphere had a higher degree centrality than the long-range network at the beginning of the stimulation, which was reversed by the end of stimulation duration. The comprehensive nodal analysis showed that, under stimulation, the degree centrality was higher for the nodes within the same hemisphere. A higher nodal degree centrality indicates that neuronal firing under that node is harmonized with the neuronal circuits of various regions.

Owing to the advancements in clinical neuroscience, the brain regions responsible for various diseases are being identified. The nodal results of degree centrality indicate that the rehabilitation of a targeted brain region can be achieved by using a similar montage for stimulation. The connection density considers network size along with the number of connections in a network to highlight the ROI. The connection density, as expected, improved for all networks because of the neuroplasticity induced by brain stimulation. However, the network density does not exemplify the clustering capacity of the network. The clustering coefficient showed marginal improvements during the stimulation for the short-range network and the complete prefrontal network. It is compelling that the increase in the number of connections does not change the clustering coefficient. This shows that the new connections are widely distributed in these networks. The unstimulated hemisphere showed a slight improvement, whereas the long-range network showed a significant increase in the clustering coefficient. The local efficiency is higher when there are clusters in a network. The results of this study indicated a similar clustering coefficient and local efficiency. The nodal efficiency of the short-range network of the right hemisphere showed higher values for the nodes under stimulation than the remaining nodes in the same network. The global efficiency exhibited an equal increase for all networks, except for the long-range network, which showed a more progressive response to stimulation. The modularity of the complete prefrontal and stimulated networks illustrated a decline with an increase in the stimulation period. The stimulated hemisphere showed a rapid decline of modularity in the initial 7 min but remained almost identical for the remaining 3 min. The modularity exhibited a trend opposite to that of degree centrality, which may indicate that new connections improve the homogeneity of the network such that nodes possess a similar number of connections. The response of the short-range network of the left hemisphere and the long-range network showed a random response. The measures of assortativity and betweenness did not present meaningful

information reflecting an improvement in the brain state. A previous fNIRS study observed the varying response of assortativity and modularity, which was attributed to the nature of these metrics. The results of this study reveal that the network theory metrics of global and nodal degree centrality and efficiency and connection density can effectively indicate improvements in the brain state during stimulation sessions. Therefore, the metrics are feasible to be used in the feedback control of brain state.

The results in this paper show the feasibility of the proposed neurofeedback methodology using real-time connectivity analyses.[66] The connectivity percentage and network theory metrics can help identify the brain state. Furthermore, continuous monitoring of the brain state can help abort the stimulation once the desired improvement is achieved. The desired brain state can be determined based on a single metric or a combination of metrics by using the proposed methodology. The results of this study have shown that the nodal metrics can be computed to monitor a specifically targeted brain region along with the global metrics of a network of the desired size, which constitutes a specific brain region. This is in-line with other studies that have used functional connectivity and network theory measures to express the brain state and cognitive capability of healthy and diseased populations.[11,18,29,34] The proposed strategy is not limited to the resting state studies as the recommended network parameters are independent of the experimental paradigm. It can be exploited in recent studies where the cognitive training was augmented with tDCS to show positive results.[67] The proposed methodology can be utilized in cases where the tDCS parameters are different from the one used in this study. The tDCS effects can vary based on the electrode montage, size, and location on the head, inter-electrode distance, current intensity, and stimulation duration. The variations can increase or decrease the enhancement that will be measured by the recommended network metrics.[16,17,68] Furthermore, the changes in the brain state can be monitored robustly with the recommended parameters even if the synchronization calculation mechanism is changed.

The proposed real-time feedback methodology has an important application in the rising field of tele-neuromodulation, where subjects can have brain stimulation therapy at home.[38,41] The feedback loop, in this case, will utilize the technology advancements

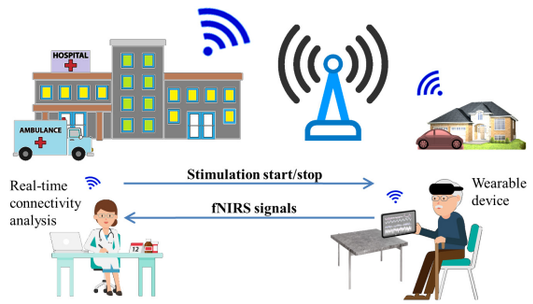

Fig. 9. The application to proposed methodology to the rising tele-neuromodulation with real-time control of stimulation duration.

in the telemedicine industry such that the therapist can supervise the stimulation protocol in real-time, as shown in Fig. 9. The desired brain state and the target brain region can be set by authorized personnel such as a doctor or psychiatrist who is familiar with the patient's condition. The therapist can then guide the patient in setting up the device, which already has the fNIRS optodes and HD-tDCS electrodes embedded in order to remove any risks of wrong placement. The therapist can control the start of the protocol and monitor the brain state. Lastly, the stimulation can be stopped by the therapist once the desired brain state is achieved. Special care must be observed in these experiments as recommended by the guideline for tele-neuromodulation and effects of stimulation.[69–72]

5. Limitations and Future Research Potential

Despite its advantages, the study has several limitations. fNIRS can only observe changes occurring in the slow metabolic correlations of brain activity. Therefore, the rapid changes occurring in the brain cannot be acquired. The setting up of separate devices can be difficult and time-consuming, especially for elderly patients who are generally more susceptible to brain stimulation. Therefore, new hybrid devices combining fNIRS and tDCS should be developed to simplify the proposed tele-neuromodulation strategy. The study also has a limited number of fNIRS channels. In the future, additional channels should be configured, and multiple brain regions should be monitored using high-density imaging at different cortices or simultaneous measurement

with electroencephalography.[28,73] In addition, short-separation channels that can improve signal quality by capturing only the physiological signal from superficial layers of the brain were not configured in this study. Therefore, future studies should incorporate these short-separation channels.

The experiment lasted for only 10 min, which is a limitation that can be avoided in future studies. Although, the targeted effect of stimulation was achieved as the right hemisphere did not show further improvement. However, the broader effect of stimulation in other regions could reach some saturation level that was not observed in this study due to 10 min of stimulation. Furthermore, the authors were not able to observe any adverse effect of stimulation on the connectivity with excessive stimulation due to limited time duration. The study lacked the presence of a placebo group that can be useful to independently claim the beneficial effects of tDCS. Therefore, a placebo group can be recruited in future studies. In this study, we only provided 1 mA of brain stimulation and did not explore the effect of various current intensities. It will be interesting to know the effect of higher current intensities in future studies.

The connectivity matrices used in this study were established using Pearson's correlation coefficient. Other methods based on wavelet phase synchronization and cross-correlation techniques can be explored, and their results can be compared to those of this study. In contrast to these approaches, Permutation Disalignment Index has been recently proposed to explore brain connectivity, which can be exploited in combination with fuzzy or multi-level logic to form a binary network.[74] These schemes may contribute to a better selection of parameters for the proposed neurofeedback methodology.

6. Conclusions

In this study, the general effect of transcranial brain stimulation and the focal effects of HD-tDCS were demonstrated by simultaneously measuring fNIRS signals to monitor improvements in the default mode network. Analyses of the complete prefrontal functional network and its subnetworks showed that connectivity was enhanced continuously throughout the stimulation duration. The increase in functional connectivity can be quantified as connectivity percentage as it is found to be in-line with the results of the network theory measures. The brain state of the targeted brain region showed significant enhancement only during the initial 7 min of stimulation. The network theory metrics of degree centrality, efficiency, and connection density can provide feedback regarding the brain state. These results support our hypothesis that the improvement in brain state cannot be further enhanced once a certain level is achieved. The proposed neurofeedback-based methodology is feasible to be implemented in real-time to control the stimulation duration. The effective stimulation duration for stimulation therapy can be determined using the closed-loop neuromodulation approach.

Conflict of Interest

The authors declare that they have no conflict of interest. This research was conducted in the absence of any commercial or financial relationship that could be construed as a potential conflict of interest.

Acknowledgments

This work was supported by the National Research Foundation (NRF) of Korea under the auspices of the Ministry of Science and ICT, Republic of Korea (Grant Nos. NRF-2020R1A2B5B03096000 and NRF-2021R1A5A1032937).

References

1. W. He, P. Y. Fong, T. W. H. Leung and Y. Z. Huang, Protocols of non-invasive brain stimulation for neuroplasticity induction, *Neurosci. Lett.* **719** (2020) 133437.
2. A. Finisguerra, R. Borgatti and C. Urgesi, Non-invasive brain stimulation for the rehabilitation of children and adolescents with neurodevelopmental disorders: A systematic review, *Front. Psychol.* **10** (2019) 135.
3. A. T. Barker, R. Jalinous and I. L. Freeston, Non-invasive magnetic stimulation of human motor cortex, *Lancet* **325** (1985) 1106–1107.
4. M. A. Nitsche and W. Paulus, Excitability changes induced in the human motor cortex by weak transcranial direct current stimulation, *J. Physiol.* **527** (2000) 633–639.
5. L. Claes, H. Stamberger, P. V. Heyning, D. D. Ridder and S. Vanneste, Auditory cortex tACS and tRNS for tinnitus: Single versus multiple sessions, *Neural Plast.* **2014** (2014) 436713.
6. M. Ortiz, E. Iáñez, J. A. Gaxiola-Tirado, D. Gutiérrez and J. M. Azorín, Study of the functional

brain connectivity and lower-limb motor imagery performance after transcranial direct current stimulation, *Int. J. Neural Syst.* **30** (2020) 2050038.
7. A. R. Brunoni, J. Amadera, B. Berbel, M. S. Volz, B. G. Rizzerio and F. A. Fregni, A systematic review on reporting and assessment of adverse effects associated with transcranial direct current stimulation, *Int. J. Neuropsychopharmacol.* **14** (2011) 1133–1145.
8. A. J. Woods, A. Antal, M. Bikson, P. S. Boggio, A. R. Brunoni, P. Celnik *et al.*, A technical guide to tDCS, and related non-invasive brain stimulation tools, *Clin. Neurophysiol.* **127** (2016) 1031–1048.
9. M. Bikson, P. Grossman, C. Thomas, A. L. Zannou, J. Jiang, T. Adnan *et al.*, Safety of transcranial direct current stimulation: Evidence based update 2016, *Brain Stimul.* **9** (2016) 641–661.
10. N. Roche, M. Geiger and B. Bussel, Mechanisms underlying transcranial direct current stimulation in rehabilitation, *Ann. Phys. Rehabil. Med.* **58** (2015) 214–219.
11. R. Polanía, M. A. Nitsche and W. Paulus, Modulating functional connectivity patterns and topological functional organization of the human brain with transcranial direct current stimulation, *Hum. Brain Mapp.* **32** (2011) 1236–1249.
12. K. T. Jones, F. Gözenman and M. E. Berryhill, The strategy and motivational influences on the beneficial effect of neurostimulation: A tDCS and fNIRS study, *Neuroimage* **105** (2015) 238–247.
13. M. Mancini, D. Brignani, S. Conforto, P. Mauri, C. Miniussi and M. C. Pellicciari, Assessing cortical synchronization during transcranial direct current stimulation: A graph-theoretical analysis, *Neuroimage* **140** (2016) 57–65.
14. A. C. Ehlis, F. B. Haeussinge, A. Gastel, A. J. Fallgatter and C. Plewnia, Task-dependent and polarity-specific effects of prefrontal transcranial direct current stimulation on cortical activation during word fluency, *Neuroimage* **140** (2016) 134–140.
15. A. C. Merzagora, G. Foffani, I. Panyavin, L. Mordillo-Mateos, J. Aguilar, B. Onaral *et al.*, Prefrontal hemodynamic changes produced by anodal direct current stimulation, *Neuroimage* **49** (2010) 2304–2310.
16. S. K. Kessler, P. Minhas, A. J. Woods, A. Rosen, C. Gorman and M. Bikson, Dosage considerations for transcranial direct current stimulation in children: A computational modeling study, *PLoS One* **8** (2013) e76112.
17. A. Datta, V. Bansal, J. Diaz, J. Patel, D. Reato and M. Bikson, Gyri-precise head model of transcranial direct current stimulation: Improved spatial focality using a ring electrode versus conventional rectangular pad, *Brain Stimul.* **2** (2009) 201–207.
18. M. A. Yaqub, S.-W. Woo and K.-S. Hong, Effects of HD-tDCS on resting-state functional connectivity in the prefrontal cortex: An fNIRS study, *Complexity* **2018** (2018) 1613402.
19. D. Edwards, M. Cortes, A. Datta and P. Minhas, E. M. Wassermann and M. Bikson, Physiological and modeling evidence for focal transcranial electrical brain stimulation in humans: A basis for high-definition tDCS, *Neuroimage* **74** (2013) 266–275.
20. H. I. Kuo, M. Bikson, A. Datta, P. Minhas, W. Paulus, M. F. Kuo *et al.*, Comparing cortical plasticity induced by conventional and high-definition 4×1 ring tDCS: A neurophysiological study, *Brain Stimul.* **6** (2013) 644–648.
21. P. Pinti, I. Tachtsidis, A. Hamilton, J. Hirsch, C. Aichelburg, S. Gilbert *et al.*, The present and future use of functional near-infrared spectroscopy (fNIRS) for cognitive neuroscience, *Ann. NY Acad. Sci.* **1464** (2020) 5–29.
22. U. Ghafoor, J. H. Lee, K.-S. Hong, S. S. Park, J. Kim and H.-R. Yoo, Effects of acupuncture therapy on MCI patients using functional near-infrared spectroscopy, *Front. Aging Neurosci.* **11** (2019) 237.
23. R. Li, G. Rui, W. Chen, S. Li, P. E. Schulz and Y. Zhang, Early detection of Alzheimer's disease using non-invasive near-infrared spectroscopy, *Front. Aging Neurosci.* **10** (2018) 366.
24. F. Herold, P. Wiegel, F. Scholkmann and N. G. Müller, Applications of functional near-infrared spectroscopy (fNIRS) neuroimaging in exercise–cognition science: A systematic, methodology-focused review, *J. Clin. Med.* **7** (2018) 466.
25. K.-S. Hong and M. A. Yaqub, Application of functional near-infrared spectroscopy in the healthcare industry: A review, *J. Innov. Opt. Health Sci.* **12** (2019) 1930012.
26. P. Arpaia, F. Donnarumma, A. Esposito and M. Parvis, Channel selection for optimal EEG measurement in motor imagery-based brain-computer interfaces, *Int. J. Neural Syst.* **31** (2021) 2150003.
27. M. N. A. Khan, M. R. Bhutta and K.-S. Hong, Task-specific stimulation duration for fNIRS brain-computer interface, *IEEE Access* **8** (2020) 89093–89105.
28. M. A. Yaqub, S.-W. Woo and K.-S. Hong, Compact, portable, high-density functional near-infrared spectroscopy system for brain imaging, *IEEE Access* **8** (2020) 128224–128238.
29. M. D. Fox and M. E. Raichle, Spontaneous fluctuations in brain activity observed with functional magnetic resonance imaging, *Nat. Rev. Neurosci.* **8** (2007) 700–711.
30. J. delEtoile and H. Adeli, Graph theory and brain connectivity in Alzheimer's disease, *Neuroscientist* **23** (2017) 616–626.
31. M. Ahmadlou and H. Adeli, Complexity of weighted graph: A new technique to investigate structural complexity of brain activities with applications to aging and autism, *Neurosci. Lett.* **650** (2017) 103–108.
32. R. Yuvaraj, M. Murugappan, U. R. Acharya, H. Adeli, N. M. Ibrahim and E. Mesquita, Brain

functional connectivity patterns for emotional state classification in Parkinson's disease patients without dementia, *Behav. Brain Res.* **298** (2016) 248–260.
33. M. Ahmadlou, A. Adeli, R. Bajo and H. Adeli, Complexity of functional connectivity networks in mild cognitive impairment subjects during a working memory task, *Clin. Neurophysiol.* **125** (2014) 694–702.
34. D. Yang, S.-H. Yoo, C.-S. Kim and K.-S. Hong, Evaluation of neural degeneration biomarkers in the prefrontal cortex for early identification of patients with mild cognitive impairment: An fNIRS study, *Front. Hum. Neurosci.* **13** (2019) 317.
35. F. S. Racz, P. Mukli, Z. Nagy and A. Eke, Increased prefrontal cortex connectivity during cognitive challenge assessed by fNIRS imaging, *Biomed. Opt. Express* **8** (2017) 3842–3855.
36. F. Miraglia, F. Vecchio, C. Marra, D. Quaranta, F. Alù, B. Peroni, G. Granata, E. Judica, M. Cotelli and P. M. Rossini, Small world index in default mode network predicts progression from mild cognitive impairment to dementia, *Int. J. Neural Syst.* **30** (2020) 2050004.
37. H. Zhu, J. Xu, J. Li, H. Peng, T. Cai, X. Li *et al.*, Decreased functional connectivity and disrupted neural network in the prefrontal cortex of affective disorders: A resting-state fNIRS study, *J. Affect. Disord.* **221** (2017) 132–144.
38. Z. Einalou, K. Maghooli, S. K. Setarehdan and A. Akin, Graph theoretical approach to functional connectivity in prefrontal cortex via fNIRS, *Neurophotonics* **4** (2017) 041407.
39. H. Niu, Z. Li, X. Liao, J. Wang, T. Zhao, N. Shu *et al.*, Test-retest reliability of graph metrics in functional brain networks: A resting-state fNIRS study, *PLoS One* **8** (2013) e72425.
40. T. O. Bergmann, Brain state-dependent brain stimulation, *Front. Psychol.* **9** (2018) 2108.
41. C. Zrenner, P. Belardinelli, F. Müller-Dahlhaus and U. Ziemann, Closed-loop neuroscience and non-invasive brain stimulation: A tale of two loops, *Front. Cell. Neurosci.* **10** (2016) 92.
42. L. E. Charvet, M. T. Shaw, M. Bikson, A. J. Woods and H. Knotkova, Supervised transcranial direct current stimulation (tDCS) at home: A guide for clinical research and practice, *Brain Stimul.* **13** (2020) 686–693.
43. B. Christie, Doctors revise declaration of Helsinki, *Br. Med. J.* **321** (2000) 913.
44. M. Muthalib, P. Besson, J. Rothwell and S. Perrey, Focal hemodynamic responses in the stimulated hemisphere during high-definition transcranial direct current stimulation, *Neuromodulation* **21** (2018) 348–354.
45. L. Kocsis, P. Herman and A. Eke, The modified Beer–Lambert law revisited, *Phys. Med. Biol.* **51** (2006) N91.
46. H. D. Nguyen and K.-S. Hong, Bundled-optode implementation for 3D imaging in functional near-infrared spectroscopy, *Biomed. Opt. Express* **7** (2016) 3491–3507.
47. H. H. Shen, Core concept: Resting-state connectivity, *Proc. Natl. Acad. Sci. USA* **112** (2015) 14115–14116.
48. M. Rubinov and O. Sporns, Complex network measures of brain connectivity: Uses and interpretations, *Neuroimage* **52** (2010) 1059–1069.
49. J. Xu, X. Liu, J. Zhang, Z. Li, X. Wang, F. Fang *et al.*, FC-NIRS: A functional connectivity analysis tool for near-infrared spectroscopy data, *Biomed. Res. Int.* **2015** (2015) 248724.
50. Z. Wang, A. C. Bovik, H. R. Sheikh and E. P. Simoncelli, Image quality assessment: From error visibility to structural similarity, *IEEE Trans. Image Process.* **13** (2004) 600–612.
51. N. Serrano, D. López-Sanz, R. Bruña, P. Garcés, I. C. Rodríguez-Rojo, A. Marcos, D. P. Crespo and F. Maestú, Spatiotemporal oscillatory patterns during working memory maintenance in mild cognitive impairment and subjective cognitive decline, *Int. J. Neural Syst.* **30** (2020) 1950019.
52. J. D. Cohen, W. M. Perlstein, T. S. Braver, L. E. Nystrom, D. C. Noll, J. Jonides *et al.*, Temporal dynamics of brain activation during a working memory task, *Nature* **386** (1997) 604–608.
53. M. Xia, F. Y. Womer, M. Chang, Y. Zhu, Q. Zhou, E. K. Edmiston *et al.*, Shared and distinct functional architectures of brain networks across psychiatric disorders, *Schizophr. Bull.* **45** (2019) 450–463.
54. S. Jiang, H. Pei, Y. Huang, Y. Chen, L. L. Liu, J. F. Li, H. He, D. Z. Yao and C. Luo, Dynamic temporospatial patterns of functional connectivity and alterations in idiopathic generalized epilepsy, *Int. J. Neural Syst.* **30** (2020) 2050065.
55. S. Fecteau, D. Knoch, F. Fregni, N. Sultani, P. Boggio and A. Pascual-Leone, Diminishing risk-taking behavior by modulating activity in the prefrontal cortex: A direct current stimulation study, *J. Neurosci.* **27** (2007) 12500–12505.
56. J. Luo, H. Ye, H. Zheng, S. Chen and D. Huang, Modulating the activity of the dorsolateral prefrontal cortex by tDCS alters distributive decisions behind the veil of ignorance via risk preference, *Behav. Brain Res.* **328** (2017) 70–80.
57. T. Bi and F. Fang, Impaired face perception in individuals with autism spectrum disorder: Insights on diagnosis and treatment, *Neurosci. Bull.* **33** (2017) 757–759.
58. N. Honzel, T. Justus and D. Swick, Posttraumatic stress disorder is associated with limited executive resources in a working memory task, *Cogn. Affect. Behav. Neurosci.* **14** (2014) 792–804.
59. M. Bogdanov and L. Schwabe, Transcranial stimulation of the dorsolateral prefrontal cortex prevents

stress-induced working memory deficits, *J. Neurosci.* **36** (2016) 1429–1437.
60. K. Ota, M. Shinya and K. Kudo, Transcranial direct current stimulation over dorsolateral prefrontal cortex modulates risk-attitude in motor decision-making, *Front. Hum. Neurosci.* **13** (2019) 297.
61. L. C. Yang, P. Ren and Y. Y. Ma, Anodal transcranial direct-current stimulation over the right dorsolateral prefrontal cortex influences emotional face perception, *Neurosci. Bull.* **34** (2018) 842–848.
62. M. Liebrand, A. Karabanov, D. Antonenko, A. Flöel, H. R. Siebner, J. Classen *et al.*, Beneficial effects of cerebellar tDCS on motor learning are associated with altered putamen-cerebellar connectivity: A simultaneous tDCS-fMRI study, *Neuroimage* **223** (2020) 117363.
63. N. R. Nissim, A. O'Shea, A. Indahlastari, R. Telles, L. Richards, E. Porges *et al.*, Effects of in-scanner bilateral frontal tDCS on functional connectivity of the working memory network in older adults, *Front. Aging Neurosci.* **11** (2019) 51.
64. E. Olejarczyk, U. Zuchowicz, A. Wozniak-Kwasniewska, M. Kaminski, D. Szekely and O. David, The impact of repetitive transcranial magnetic stimulation on functional connectivity in major depressive disorder and bipolar disorder evaluated by directed transfer function and indices based on graph theory, *Int. J. Neural Syst.* **30** (2020) 2050015.
65. E. Bullmore and O. Sporns, Complex brain networks: Graph theoretical analysis of structural and functional systems, *Nat. Rev. Neurosci.* **10** (2009) 186–198.
66. Y. Zhang and C. Zhu, Assessing brain networks by resting-state dynamic functional connectivity: An fNIRS-EEG study, *Front. Neurosci.* **13** (2020) 1430.
67. B. J. Lawrence, N. Gasson, A. R. Johnson, L. Booth and A. M. Loftus, Cognitive training and transcranial direct current stimulation for mild cognitive impairment in Parkinson's disease: A randomized controlled trial, *Parkinsons Dis.* **2018** (2018) 4318475.
68. M. M. Stecker, Transcranial electric stimulation of motor pathways: A theoretical analysis, *Comput. Biol. Med.* **35** (2005) 133–155.
69. L. E. Charvet, M. T. Shaw, M. Bikson, A. J. Woods and H. Knotkova, Supervised transcranial direct current stimulation (tDCS) at home: A guide for clinical research and practice, *Brain Stimul.* **13** (2020) 686–693.
70. G. Thut, T. O. Bergmann, F. Fröhlich, S. R. Soekadar, J.-S. Brittain, A. Valero-Cabré *et al.*, Guiding transcranial brain stimulation by EEG/MEG to interact with ongoing brain activity and associated functions: A position paper, *Clin. Neurophysiol.* **128** (2017) 843–857.
71. A. Vossen, J. Gross and G. Thut, Alpha power increase after transcranial alternating current stimulation at alpha frequency (α-tACS) reflects plastic changes rather than entrainment, *Brain Stim.* **8** (2015) 499–508.
72. D. Veniero, A. Vossen, J. Gross and G. Thut, Lasting EEG/MEG aftereffects of rhythmic transcranial brain stimulation: Level of control over oscillatory network activity, *Front. Cell. Neurosci.* **9** (2015) 477.
73. C. T. Lin, J. T. King, C. H. Chuang, W. P. Ding, W. Y. Chuang, L. D. Liao and Y. K. Wang, Exploring the brain responses to driving fatigue through simultaneous EEG and fNIRS measurements, *Int. J. Neural Syst.* **30** (2020) 1950018.
74. J. P. Amezquita-Sanchez, N. Mammone, F. C. Morabito and H. Adeli, A new dispersion entropy and fuzzy logic system methodology for automated classification of dementia stages using electroencephalograms, *Clin. Neurol. Neurosurg.* **201** (2021) 106446.